Molecular Pharmacology Fast Forward. Published on April 1, 2016 as DOI: 10.1124/mol.115.102434
This article has not been copyedited and formatted. The final version may differ from this version.

MOL #102434

Inhibition of GLI1 Expression by Targeting the CRD-BP-GLI1 mRNA Interaction Using Specific Oligonucleotide

Kashif Mehmood, Daud Akhtar, Sebastian Mackedenski, Chuyi Wang, and Chow H. Lee

Chemistry Program (K.M., D.A., S.M., C.W., C.H.L), University of Northern British Columbia, 3333 University Way, Prince George, British Columbia V2N 4Z9, Canada

Molecular Pharmacology Fast Forward. Published on April 1, 2016 as DOI: 10.1124/mol.115.102434
This article has not been copyedited and formatted. The final version may differ from this version.

CRD-BP-GLI1 RNA Interaction Inhibited by Oligonucleotide

Corresponding author:

Chow H. Lee, Chemistry Program, University of Northern British Columbia, 3333 University Way, Prince George, British Columbia V2N 4Z9, Canada.

Tel: 250-960-5413; Fax: 250-960-5170; Email: chow.lee@unbc.ca

Number of text pages: 31

Number of tables: 2

Number of figures: 8

Number of references: 26

Number of words in the Abstract: 244

Number of words in the Introduction: 580

Number of words in the Discussion: 1388

ABBREVIATIONS: CRD-BP, coding region determinant-binding protein; EMSA, electrophoretic mobility shift assay; KH domain, heterogeneous nuclear ribonucleoprotein-K-homology domain; Hh, hedgehog; SMO, smoothened; nts, nucleotides; TAMRA, 5-carboxytetramethylrhodamine; qRT-PCR, quantitative real time-polymerase chain reaction; K_d, dissociation constant.

Molecular Pharmacology Fast Forward. Published on April 1, 2016 as DOI: 10.1124/mol.115.102434
This article has not been copyedited and formatted. The final version may differ from this version.

ABSTRACT

The stabilization of GLI1 mRNA by Coding Region Determinant-Binding Protein (CRD-BP) through the Wnt/β-catenin signaling pathway is implicated in the proliferation of colorectal cancer and basal cell carcinoma. Here, we set out to characterize the physical interaction between CRD-BP and GLI1 mRNA so as to find inhibitors for such interaction. Studies using CRD-BP variants with a point mutation in the GXXG motif at each KH domain showed that KH1 and KH2 domain are critical for the binding of GLI1 RNA. The smallest region of GLI1 RNA binding to CRD-BP was mapped to nts 320-380. A 37-nt S1 RNA sense oligonucleotide, containing two distinct stem loops present in nts 320-380 of GLI1 RNA, was found to be effective in blocking CRD-BP-GLI1 RNA interaction. Studies using various competitor RNAs with modifications to S1 RNA oligonucleotide further displayed that both the sequences and the structure of the two stem loops are important for CRD-BP-GLI1 RNA binding. The role of the two stem loop motif in influencing CRD-BP-RNA interaction was further investigated in cells. The 2'-*O*-methyl derivative of the S1 RNA oligonucleotide significantly decreased GLI1, c-*myc* and CD44 mRNA levels, in a panel of colon and breast cancer cells. The results from this study demonstrate the potential importance of the two-stem loop motif as a target region for the inhibition of the CRD-BP-GLI1 RNA interaction and Hh signaling pathway. Such results pave the way for the development of novel inhibitors which act by destabilizing the CRD-BP-GLI1 mRNA interaction.

Molecular Pharmacology Fast Forward. Published on April 1, 2016 as DOI: 10.1124/mol.115.102434
This article has not been copyedited and formatted. The final version may differ from this version.

Introduction

The Hedgehog (Hh) signaling pathway plays a crucial role in embryonic development and cell homeostasis (Hui and Angers, 2011). Its aberrant activation has been linked to tumorigenesis (Hui and Angers, 2011; Amakye et al., 2013). For instance, mutations in the key protein components leading to the constitutive activation of the Hh pathway have been identified in medulloblastoma and basal cell carcinoma (Scales and de Sauvage, 2009). In addition, exaggerated Hh signaling in the absence of known driver mutations has been linked to many types of cancers, including colon, breast, pancreatic, gastric, lung and prostate cancers, as well as leukemia and multiple myeloma (Scales and Sauvage, 2009). Key components of the mammalian Hh pathway include a positive regulatory transmembrane protein Smoothened (SMO) and the glioma-associated oncogene (GLI) zinc finger transcription factors (GLI1, GLI2 and GLI3), with GLI1 being predominantly a transcriptional activator (Hui and Angers, 2011). While GLI1 mRNA level is widely accepted as an indicator of Hh pathway activity, GLI signaling can also be regulated by proteins involved in other signaling pathways. For instance, it has recently been shown that Wnt/β-catenin signaling can elevate GLI1 expression and transcriptional activity through the induction of expression of an RNA-binding protein called CRD-BP which acts by binding to and stabilizing GLI1 mRNA (Noubissi et al., 2009). This mode of GLI1 regulation appears to be important for the survival and proliferation of colorectal cancer and basal cell carcinoma cells (Noubissi et al., 2009 and 2014).

Coding region determinant-binding protein (CRD-BP) belongs to a highly conserved family of RNA-binding proteins which have two N-terminal RNA recognition motifs (RRM) followed by four C-terminal heterogeneous nuclear RNP-K-homology (KH) domains (Bell et al., 2013). In addition to GLI1, CRD-BP also has high affinity for several mRNAs whose protein products

Molecular Pharmacology Fast Forward. Published on April 1, 2016 as DOI: 10.1124/mol.115.102434
This article has not been copyedited and formatted. The final version may differ from this version.

have been implicated in cancer. These include mRNAs for c-*myc* (Prokipcak et al., 1994), CD44 (Vikesaa et al., 2006; King et al., 2014), K-Ras (Mongroo et al., 2011), βTrCP1 (Noubissi et al., 2006), MITF (Goswami et al., 2015), MAPK4 (Stohr et al., 2012), β-catenin (Gu et al., 2008) and MDR1 (Sparanese and Lee, 2007). The role of CRD-BP in cancer is further supported by the following findings: (i) overexpression of CRD-BP in various human cancers which include colon and breast cancers (Bell et al., 2013), and (ii) mice genetically engineered to overproduce CRD-BP in their mammary glands developed mammary adenocarcinoma (Tessier et al., 2004). Studies on various mRNA targets of CRD-BP have now confirmed that the oncogenic function of CRD-BP is due to its physical association with the corresponding mRNAs leading to their stabilization, increased expression, and ultimately the presentation of the cancerous phenotypes (Vikesaa et al., 2006; Noubissi et al., 2006 and 2009; Gu et al., 2008; Mongroo et al., 2011). Hence, the ability to disrupt specific CRD-BP-RNA interaction could represent a novel therapeutic approach for the treatment of cancer.

We recently characterized CRD-BP-CD44 RNA interaction and showed that specific antisense oligonucleotides which disrupt CRD-BP-CD44 RNA interaction *in vitro* can indeed suppress CD44 mRNA expression in cells (King et al., 2014). In the present study, we characterized CRD-BP-GLI1 RNA interaction *in vitro* by first mapping the smallest GLI1 RNA that can still bind CRD-BP. Based on this information, we designed a 37-nt sense RNA oligonucleotide S1 as a potential competitor and hence an inhibitor of CRD-BP-GLI1 RNA interaction. We demonstrate that S1 RNA oligonucleotide can effectively inhibit CRD-BP-GLI1 RNA interaction *in vitro* and can suppress GLI1 mRNA expression in a panel of human colon and breast cancer cells.

Molecular Pharmacology Fast Forward. Published on April 1, 2016 as DOI: 10.1124/mol.115.102434
This article has not been copyedited and formatted. The final version may differ from this version.

Materials and Methods

Cell Culture. Colon cancer (HCT116 and HT29) and breast cancer (MCF-7, MDA-MB-231 and T47D) cell lines purchased from the American Type Culture Collection (ATCC) (Rockville, Maryland) were maintained in Minimal Essential Media (Life Technologies, Burlington, Ontario) supplemented with 10% fetal bovine serum in a humidified incubator at 37°C supplied with 5% CO_2. Upon receipt of cells from ATCC, cells were immediately expanded and frozen in liquid nitrogen in large batches and used for up to 10 passages only (approximately 3 months). Cells were routinely maintained in 25 cm^2 or 75 cm^2 tissue culture flasks and harvested by 0.25% trypsin/0.02% EDTA treatment when they were in the logarithmic phase of growth for various experiments.

Oligonucleotides and Primers. Table 1 shows sequences of oligonucleotides (S1 to S8 RNA Oligo and D1 DNA Oligo) used in this study. Oligonucleotides used for the electrophoretic mobility shift assays were standard phosphodiester derivatives (Integrated DNA Technologies Inc.). For studies in cells, the RNA oligonucleotides were synthesized as 2'-*O*-methyl derivatives with a phosphodiester backbone (Integrated DNA Technologies Inc.). Table 2 shows the sequences of primers used to amplify the DNA template for use in synthesizing all the GLI1 RNA fragments described in Figs. 1 and 2.

Generation and Purification of Recombinant CRD-BP and Its Variants. The pET28b(+)-CRD-BP variant plasmids had been previously constructed (Barnes et al., 2015). Recombinant CRD-BP was purified from *Escherichia coli* BL21 (DE3) using a 1 mL bed volume of nickel-NTA (QIAGEN) column under denaturing conditions. Proteins eluted from the column at pH 5.4 were subjected to three steps of dialysis. The first step was for 24 h in a pH 7.4 buffer containing 200 mM NaCl, 20 mM Tris-HCl, 1 mM reduced glutathione, 0.1 mM oxidized glutathione, 10%

Molecular Pharmacology Fast Forward. Published on April 1, 2016 as DOI: 10.1124/mol.115.102434
This article has not been copyedited and formatted. The final version may differ from this version.

(v/v) glycerol, 2 M urea, and 0.01% (v/v) Triton X-100. The protein was then dialyzed twice, each for 2 hours in the same buffer as above but without urea and the glutathiones. Following dialysis, samples were centrifuged at 13,200 rpm for 30 min to remove any precipitated proteins. The purified protein solutions were quantified and analyzed for purity using Coomassie brilliant blue-stained 12% SDS-PAGE (Barnes et al., 2015).

Generation of DNA Templates and Radiolabeled *In-Vitro* Transcription. The human GLI1 cDNA (Accession # BC013000) purchased from Open Biosystems GE Dharmacon (Lafayette, CO) was used as a template for the generation of PCR-amplified GLI1 DNA fragments. The different sets of forward and reverse primers used to amplify the different regions of GLI1 cDNA are shown in Table 2. PCR amplified DNA templates were used directly for *in-vitro* transcription by T7 RNA polymerase. One µg of DNA template was incubated for 1 h at 37°C in a 20-µl reaction containing 1 x transcription buffer (Promega, Madison, Wisconsin), 10 mM dithiothreitol, 1 unit RNasin (Promega), 0.5 mM ATP, 0.5 mM CTP, 0.5 mM GTP, 12.5 µM UTP, 1.5 units T7 RNA polymerase (Promega, Madison, WI), and 40 µCi [α-^{32}P] UTP (3000 Ci/mmol). Following incubation, 3 units of RNase-free DNase I (Promega) were added and the reaction was further incubated for 10 min at 37°C. Upon addition of 10 µl Stopping dye (9 M urea, 0.01% bromophenol blue, 0.01% xylene cyanole FF, 0.01% phenol), the entire sample was electrophoresed on a 8% polyacrylamide/7M urea gel and the band containing internally-radiolabeled RNA was excised and eluted with elution buffer (10 mM Tris-HCl pH 7.5, 0.1M NaCl, 1 mM EDTA, 0.01% SDS) at 45^{0}C for 6 hours. The purified, radiolabeled RNA was then phenol/chloroform extracted followed by ethanol precipitation. Specific activity of the RNA was then determined by scintillation counting.

Generation of Unlabeled RNA. For the synthesis of unlabeled GLI1 RNA nts 230-420, 420-610 and 320-380 for use in competitive electrophoretic mobility shift assay, the following

Molecular Pharmacology Fast Forward. Published on April 1, 2016 as DOI: 10.1124/mol.115.102434
This article has not been copyedited and formatted. The final version may differ from this version.

reactions and procedures were taken. Each *in-vitro* transcription reaction contained 5 μg of gel purified DNA template, 10 μL 10 x T7 buffer (400 mM Tris-HCl pH 7.6, 240 mM $MgCl_2$, 20 mM spermidine, 0.1% Triton X-100), 5 μL each of 100 mM ATP, CTP, GTP, and UTP, 40 units RNasin, 5 units of T7 RNA polymerase to a total volume of 100 μL. The reaction was incubated at 37°C overnight and then treated with DNase I to remove the DNA template. Phenol-chloroform extraction was performed to remove protein impurities followed by passing through G-50 spin column to remove unincorporated nucleotides. RNA was then ethanol precipitated and re-suspended in DEPC-treated water. The purity of RNA was examined by visualization on 2.5% agarose gel, and their concentrations were determined using a spectrophotometer.

Electrophoretic Mobility Shift Assay. The electrophoretic mobility shift assay (EMSA) was conducted in essentially the same manner as previously described (King et al., 2014; Barnes et al., 2015). The EMSA competition assays involved the pre-incubation between competitor molecules (oligonucleotides or RNA) and 300 nM CRD-BP for 10 minutes at 35°C. Following the pre-incubation, 13 nM [^{32}P]-labelled *GLI* RNA nts 230-420 was added to the reaction. This was followed by the standard EMSA protocol. The molar excess concentrations of oligonucleotides or RNA over the [^{32}P]-labelled *GLI* RNA are shown in Fig. 5.

Cell Transfection. Cells were plated in 6-well plates at a density of 2.5×10^4 cells/mL. After 20 h, cells were transfected with 20 nM of double-stranded Dicer substrate RNAi (dsRNAi) which was directed against CRD-BP mRNA (Integrated DNA Technologies Inc.) using Lipofectamine 2000 reagent (Life Technologies Inc.). The sense and antisense sequences were: r(GGAGGAGAACUUCUUUGGUCCCA)dAG and r(CUUGGGACCAAAGAAGUUCUCCUCCUU). As a negative control, cells were transfected

Molecular Pharmacology Fast Forward. Published on April 1, 2016 as DOI: 10.1124/mol.115.102434
This article has not been copyedited and formatted. The final version may differ from this version.

with the negative control duplex NC1 (Integrated DNA Technologies Inc.). After a 48 h incubation, cells from duplicate wells were subjected to RNA isolation as described below.

RNA Isolation and Quantitative Real-Time PCR. Total RNA was extracted from cells using the *mir*Vana™ miRNA Isolation Kit (Ambion Inc.) as according to the manufacturer's instructions. GLI1, CD44, c-*myc,* KRas and β–actin mRNA levels were examined by quantitative real-time PCR (qRT-PCR). After removing DNA using DNA Free kit (Ambion Inc.), the first strand of cDNA synthesis was performed using iScript cDNA synthesis kit (Bio-Rad, Mississauga, Ontario) on 1 μg of total RNA. Following cDNA synthesis, qRT-PCR reactions of GLI1, c-*myc,* KRas and β–actin mRNAs were carried out using iQ SYBR Green Supermix (Bio-Rad) on an iQ5 Real-Time PCR Detection System (Bio-Rad). The GLI1 PCR primers which have been successfully used by others (Noubissi et al., 2009) were: GLI1forward primer, 5'-CCC AAT CAC AAG TCA GGT TCC T-3', and GLI1 reverse primer, 5'-CCT ATG TGA AGC CCT ATT TGC C-3'. Specificity was confirmed by performing melt-curve analysis. The PCR primers used for measuring CD44, c-*myc,* and β-actin mRNA levels using the SYBR Green method have been previously described (King et al., 2014; Barnes et al., 2015). The cycling protocol consisted of 95°C for 3 min and 40 cycles of denaturation at 95°C for 10 s, and annealing at 52°C for 30 s. For measuring CRD-BP mRNA level, the iQ supermix (BioRad) and Fam-TAMRA probe were used. The PCR primers and Fam-TAMRA labeled probe included the following: CRD-BP forward primer, 5'-AAC CCT GAG AGG ACC ATC ACT-3', CRD-BP reverse primer, 5'-AGC TGG GAA AAG ACC TAC AGC-3', and CRD-BP Taqman probe, 5'-/56-FAM/TGT TGC AGG GCC GAG CAG GA/36-TAMSp/-3'(Kato et al., 2007); β–actin forward primer. 5'-TTG CCG ACA GGA TGC AGA AGG A-3', β–actin reverse primer, 5'-AGG TGG ACA GCG AGG CCA GGA T-3', and β–actin Taqman probe, 5'-/56 FAM/ATG AAG ATC AAG ATC ATT GCT CCT

Molecular Pharmacology Fast Forward. Published on April 1, 2016 as DOI: 10.1124/mol.115.102434
This article has not been copyedited and formatted. The final version may differ from this version.

CCT G/36-TAMSp/-3'. The cycling protocol was designed with following specifications: 95°C for 2 min, 40 cycles of denaturation at 95°C for 45 s, annealing at 53°C for 30 s. Each sample was tested in triplicate, and the data was analyzed using iQ5 optical system software. The C_T values for target genes (GLI1, CD44, CRD-BP, and c-*myc*) and reference gene (β-actin) were then used in the comparative C_T method or commonly known as the $2^{-\Delta\Delta CT}$ method (Schmittegen and Livak, 2008) to determine the expression level of a target gene in treated samples relative to the control NC1-treated samples. One-way ANOVA was performed as statistical analysis to compare the target mRNA levels (GLI1, CD44, c-*myc*, and CRD-BP) of treated sample (siRNA- or S1-treated) with the negative control (NC1- or S4-treated) after normalization to the reference gene, β-actin.

Molecular Pharmacology Fast Forward. Published on April 1, 2016 as DOI: 10.1124/mol.115.102434
This article has not been copyedited and formatted. The final version may differ from this version.

Results

Mapping the GLI1 RNA Region that Interacts with CRD-BP. Using UV cross-linking coupled with immuno-precipitation of anti-FLAG CRD-BP, it was previously shown that CRD-BP has the strongest affinity for GLI1 mRNA within its coding region at nts 41-990 (Noubissi et al., 2009). To map the region within the first 990 nts of GLI1 mRNA that binds CRD-BP, we generated 5 RNA fragments of about 200-nt in size which span nts 36-990 of GLI1 mRNA. The 5 RNA fragments span GLI1 mRNA at the following nts: 36-231, 230-420, 420-610, 610-800, and 800-990 (Fig. 1A). The results of the electrophoretic mobility shift assay in assessing these 5 radiolabeled GLI1 RNA fragments in binding to the recombinant CRD-BP are shown in Fig. 2A. As shown in Fig. 2A, the ^{32}P-labeled c-*myc* CRD RNA nts 1705-1886 which has a high affinity for CRD-BP (Barnes et al., 2015) resulted in protein-RNA complex. Amongst the 5 GLI1 RNA fragments examined, only GLI1 RNA nts 230-420 showed affinity for CRD-BP (Fig. 2A). We found that some free RNAs, including GLI1 36-230 (Fig. 1A), exhibited more than one band on non-denaturing gel. We speculate that this could be the result of an alternative structure of the particular RNA or the formation of dimer RNA. We also noticed that some RNAs are more difficult to radiolabel such as GLI1 610-800 and GLI1 800-990 (Fig. 1A). This could be the result of unusual secondary structure of RNA and/or the presence of low number of U residues. For instance, GLI1 800-990 has 29 U residues while GLI1 230-420 and GLI1 420-610 have 45 and 41 U residues respectively. We further mapped the region within nts 230-420 which is responsible for binding to CRD-BP. To do so, 4 GLI1 RNA fragments truncated from the 3' end (Fig. 1B) and 4 RNA fragments truncated from the 5' end were generated (Fig. 1C). Results of the EMSA in assessing their affinity for CRD-BP are shown in Fig. 2B and C respectively. Amongst the 3' end truncated fragments, only the RNA fragment corresponding to nts 230-380

Molecular Pharmacology Fast Forward. Published on April 1, 2016 as DOI: 10.1124/mol.115.102434
This article has not been copyedited and formatted. The final version may differ from this version.

displayed CRD-BP binding (Fig. 2B). On the other hand, we demonstrated that the three 5' end RNA truncated fragments, nts 270-420, 320-420 and 350-420, had an affinity for CRD-BP (Fig. 2C). The combined experimental data from 3' end and 5' end truncated GLI1 RNA fragments suggests that the RNA region corresponding to nts 320-380 may be the smallest affinity site required for CRD-BP binding. To test this hypothesis, a GLI1 RNA fragment nts 320-380 was generated and then assessed using EMSA. As shown in Fig. 2D, CRD-BP does indeed have an affinity for this RNA fragment. The right panel in Fig. 1 summarizes the CRD-BP binding profiles of the GLI1 RNA fragments conducted in this study.

Assessing Oligonucleotides for Ability to Inhibit the CRD-BP-GLI1 RNA Interaction. To determine if there is a distinct RNA structure present within the GLI1 RNA region that binds CRD-BP, the predicted RNA secondary structure of GLI1 nts 301-380 was generated using MFOLD (Zuker, 2003). Interestingly, the structure contains two distinct stem loops within nts 346-382 (Fig. 3). This structure is remarkably similar to the two stem loops generated for the secondary structure of CD44 RNA nts 2862-2930 (Fig. 3) which has previously been shown to have an affinity to CRD-BP (King et al., 2014). To test the hypothesis that the secondary structure, particularly the two stem loops, as well as the sequence of GLI1 RNA are critical in binding CRD-BP, 8 RNAs and 1 DNA oligonucleotides of 37-nt were designed. The predicted secondary structures of these oligonucleotides were generated using MFOLD (Fig. 4). These sense oligonucleotides with identical lengths were designed to have different structures as well as slight variations in their nucleotide sequences as shown in Table 1. The sense S1 RNA oligonucleotide corresponds to GLI1 RNA nts 346-382 while the sense D1 DNA oligonucleotide is its DNA counterpart (Fig. 4). S2, S3, S4, S5 and S6 RNA oligonucleotides were designed with variations that included the removal of each loop (S2 and S3), different loop size (S4, S5, S6) or altered distance between loops (S4) so as to determine the importance of both stem loops in

Molecular Pharmacology Fast Forward. Published on April 1, 2016 as DOI: 10.1124/mol.115.102434
This article has not been copyedited and formatted. The final version may differ from this version.

CRD-BP binding. The S7 RNA oligonucleotide was designed to determine the importance of both stems in binding CRD-BP by altering the sequence at the stem, while S8 RNA oligonucleotide was designed to test the importance of the sequence within the loop. The ability of these oligonucleotides to compete with [^{32}P]-labeled GLI1 RNA nts 230-420 for binding to CRD-BP is shown in Fig. 5. As expected, the *in-vitro* transcribed unlabeled GLI1 RNA nts 320-380 competed effectively (Fig. 5A). At 3 μM, the binding of [^{32}P] GLI1 RNA nts 230-420 was inhibited by 74% while at 22 μM, the binding was inhibited by 87%. As shown in Fig. 5A and B, the S1 RNA oligo was able to inhibit [^{32}P] GLI1 RNA binding by 89% at 147 μM. In contrast, the D1 oligo, a DNA oligonucleotide version of S1 RNA oligo, had no effect up to 147 μM which indicates that the competition observed is RNA-specific and that the D1 oligonucleotide has no affinity for CRD-BP. The S2 RNA oligonucleotide which is missing stem loop 1 at the 5' end (Fig. 4) effectively competed and inhibited CRD-BP binding by 40% at 147 μM, while the S3 RNA oligonucleotide missing stem loop 2 at the 3'end (Fig. 4) inhibited binding by 56% at similar concentration (Fig. 5B). Such reduced effectiveness suggests that the presence of both stem loops is important for binding to CRD-BP. To determine whether the size of the loop region of both stem loops is important, we designed and assessed S5 and S6 RNA oligonucleotides. The S5 RNA oligonucleotide with the smaller size loop at stem loop 1 (Fig. 4) effectively inhibited CRD-BP binding by 76% at 147 μM (Fig. 5B). On the other hand, the S6 RNA oligonucleotide containing a smaller size loop at stem loop 2 (Fig. 4) was markedly less effective as it only inhibited CRD-BP binding by 16% at a similar concentration (Fig. 5B). These results suggest that the size of loops at both stem loops is important and that stem loop 2 likely plays a more important role in binding to CRD-BP. To determine if the distance between the two stem loops is important, we designed S4 RNA oligonucleotide. In contrast to S5 RNA oligonucleotide which

Molecular Pharmacology Fast Forward. Published on April 1, 2016 as DOI: 10.1124/mol.115.102434
This article has not been copyedited and formatted. The final version may differ from this version.

has 3 nts in between stem loop 1 and 2, S4 RNA oligonucleotide which contains 6 nts in between stem loop 1 and 2 (Fig. 4) was completely ineffective as a competitor (Fig. 5B). This suggests that the close proximity of the two stem loops is critical for CRD-BP-RNA binding. Finally, we assessed the significance of sequences at the stem regions and at the loop regions in binding CRD-BP. S7 RNA oligonucleotide has similar secondary structure as S1 RNA oligonucleotide but differed only in the sequences at the two stem regions (Fig. 4). S8 RNA oligonucleotide also retained similar secondary structure as S1 RNA oligonucleotide but differed in the sequences in the loop regions (Fig. 4). As shown in Fig. 5B, S7 RNA oligonucleotide was completely ineffective while S8 RNA oligo only inhibited CRD-BP binding by 16% at 147 μM, suggesting that sequences at both the stem and loop regions are also important for CRD-BP binding.

Effect of Point Mutation in the GXXG Motif of KH Domains on the Ability of CRD-BP to bind GLI1 RNA. Using site-directed mutagenesis to mutate the first glycine to an aspartate in the GXXG motif of KH domains, we recently demonstrated that at least two KH domains of CRD-BP participate in binding c-*myc* and CD44 RNAs (Barnes et al., 2015). Here, we wished to further characterize CRD-BP-RNA interaction by determining whether CRD-BP has similar requirements for binding the GLI1 RNA. The previously described single point-mutation KH variants (KH1, KH2, KH3, and KH4) and double point-mutation KH variants (KH1-2, KH1-3, KH1-4, KH2-3, KH2-4, and KH3-4) were used in this study (Barnes et al., 2015). As additional controls, a Y5A variant which has a point mutation in the RRM1 domain and a D526E variant with a point mutation in the variable loop located between β_2 and β_3 in KH4 domain were used (Barnes et al., 2015). The representative results of electrophoretic mobility shift assay in assessing these variants for binding to [^{32}P]-labeled GLI1 RNA nts 230-420 are shown in Fig. 6A, and the data summarized from three biological replicates is shown in Fig. 6B. Both control

Molecular Pharmacology Fast Forward. Published on April 1, 2016 as DOI: 10.1124/mol.115.102434
This article has not been copyedited and formatted. The final version may differ from this version.

variants, Y5A and D526E, exhibited a dissociation constant, K_d, which is comparable to that of the WT CRD-BP. Surprisingly, the KH2 variant could not bind to GLI1 RNA while the KH1 variant demonstrated significantly weak binding and its K_d could not be determined (Fig. 6B). The KH3 variant displayed a binding profile similar to that of WT CRD-BP while the KH4 variant appeared to have a higher affinity for GLI1 RNA (Fig. 6B). All the double point-mutation KH variants, including the KH3-4 variant, displayed inability to bind to GLI1 RNA.

Effect of Knocking Down CRD-BP on GLI1 and Other mRNA Expression in Breast and Colon Cancer Cells. To further characterize CRD-BP-GLI1 RNA interaction and the downstream implications of this interaction, the ability of S1 RNA oligonucleotide to down regulate GLI1 mRNA expression was assessed. Firstly, we need to find cell line models where the CRD-BP-mRNA interaction exists. To do this, we used a double-stranded Dicer substrate RNAi (dsRNAi) directed against CRD-BP based on siRNA sequences previously shown to successfully knock down CRD-BP (Kato et al., 2007). The dsRNAi directed against CRD-BP had no effect on the level of β–actin mRNA in all cell lines tested and hence it was used as a reference gene for normalization. Cells transfected with the negative control duplex NC1 were used as controls and the mRNA levels of all genes were expressed relative to the level in NC1-treated cells. As shown in Fig. 7, the dsRNAi directed against CRD-BP was effective in knocking down CRD-BP mRNA in two colon cancer cell lines, HCT116 and HT29, and three breast cancer cell lines, MCF-7, MDA-MB-231 and T47D. The knockdown appears to be most effective in HT29, MDA-MB-231 and T47D cells where the level of CRD-BP mRNA was reduced down to 20% or less. The knockdown of CRD-BP mRNA levels in HCT116 and MCF-7 cells was reduced to 45% and 38% respectively. We found that the C_T values of CRD-BP mRNA obtained in all NC1-treated cell lines were not significantly different. In the colon cancer (HCT116 and HT29) CRD-BP-knocked down cells, the GLI1 mRNA levels were significantly suppressed

Molecular Pharmacology Fast Forward. Published on April 1, 2016 as DOI: 10.1124/mol.115.102434
This article has not been copyedited and formatted. The final version may differ from this version.

where reduction to 35-38% was observed (Fig. 7). GLI1 mRNA was also suppressed down to similar levels in the three breast cancer cell lines (Fig. 7). These results suggest that the CRD-BP-GLI1 mRNA interaction clearly exist in the colon and breast cancer cells. C-*myc* and CD44 mRNAs which are also targets of CRD-BP (Vikesaa et al., 2006; Barnes et al., 2015) were also measured to confirm the CRD-BP-RNA interaction in the CRD-BP-knocked down cells. Our results showed that a significant down-regulation of both c-*myc* and CD44 mRNA is observed in all five cell lines when CRD-BP was knocked down (Fig. 7).

Effect of S1 RNA Oligonucleotide on GLI1 and Other mRNA Expression in Breast and Colon Cancer Cells. Having shown that the physical interaction between CRD-BP and its target mRNAs exists in the cell lines studied above and based on the hypothesis that CRD-BP binds to and protects GLI1 mRNA from degradation, we next tested the ability of S1 RNA oligonucleotide, an effective competitor of CRD-BP-GLI1 RNA interaction *in vitro* (Fig. 5), to influence GLI1 mRNA levels. The 2′-*O*-methyl modified version of S1 RNA oligonucleotides was used. As a negative control, 2′-*O*-methyl modified S4 RNA oligonucleotide was used because the S4 RNA oligonucleotide is not an inhibitor of the CRD-BP-GLI1 RNA interaction (Fig. 5B). Our results showed that S4 RNA oligonucleotide had no effect on β–actin, GLI1, c-*myc*, and CD44 mRNA levels as compared to NC1-treated cells (data not shown). Hence, we normalized S1-treated mRNA level to that of S4-treated cells. The results in Fig. 8 show that S1 RNA oligonucleotide was indeed effective in suppressing GLI1 mRNA expression in all five cell lines. S1 RNA oligonucleotide was most effective in the two breast cancer cell lines MDA-MB-213 and T47D where suppression to 18% and 25% was observed (Fig. 8). The suppression of GLI1 mRNA levels down to 30% and 35% was observed in HT29 and MCF-7 cells respectively (Fig. 8), Though still statistically significant, the RNA oligonucleotide appears to be less effective in suppressing GLI1 mRNA in HCT116 cells with an inhibition of only 59%. To

Molecular Pharmacology Fast Forward. Published on April 1, 2016 as DOI: 10.1124/mol.115.102434
This article has not been copyedited and formatted. The final version may differ from this version.

investigate whether the S1 RNA oligonucleotide is specific for suppressing GLI1 mRNA or whether it can inhibit the general CRD-BP-RNA interaction leading to suppression of other CRD-BP mRNA targets, we also measured the levels of c-*myc* and CD44 mRNAs in S1-treated cells. Our results show significant down-regulation of c-*myc* mRNA, although to a lesser extent than GLI1 mRNA, in HCT116, MCF-7, MDA-MB-231 and T47D cells transfected with the S1 RNA oligonucleotide (Fig. 8). CD44 mRNA level was also significantly down-regulated in all cell lines as compared to the control S4-treated cells (Fig. 8). But it is clear that S1 RNA oligonucleotide is less effective in down-regulating CD44 mRNA because suppression down to 60-70% is observed in all the cell lines. We found that there was no effect on KRas mRNA level in cells transfected with S1 RNA oligonucleotide (data not shown). These results imply that the S1 RNA oligonucleotide which targeted CRD-BP-GLI1 RNA interaction has some level of specificity in targeting the GLI1 mRNA expression in cells but also supports the hypothesis regarding the potential importance of the distinct two stem loop motif as a region for targeted therapy.

Molecular Pharmacology Fast Forward. Published on April 1, 2016 as DOI: 10.1124/mol.115.102434
This article has not been copyedited and formatted. The final version may differ from this version.

Discussion

There is now significant cumulative evidence to implicate CRD-BP in tumour progression. While the mechanism by which CRD-BP exerts its oncogenic function is still unknown, it has become increasingly clear that its ability to physically associate with its target mRNAs is one important criterion. To date, there have been only a few studies which describe the use of molecules capable of blocking the CRD-BP-RNA interaction (Coulis et al., 2000; Mao et al., 2006; King et al., 2014; Mahapatra et al., 2014), but none have specifically described potential inhibitors of the CRD-BP-GLI1 mRNA interaction. In this study, we further characterize the CRD-BP-GLI1 RNA interaction and report that a sense RNA oligonucleotide specifically designed based on the two stem loop motif region mapped in GLI1 mRNA nts 320-380 is not only capable of blocking CRD-BP-GLI1 RNA interaction *in vitro*, but also able to inhibit GLI1 mRNA expression in a panel of colon and breast cancer cells.

Based on a previously reported study that CRD-BP has a high affinity for nts 41-990 in the coding region of GLI1 mRNA (Noubissi et al., 2009), we proceeded to map the smallest nucleotide sequence within this region which CRD-BP still binds to. Using electrophoretic mobility shift assay, we found that the 61 nts GLI1 RNA fragment spanning the coding region nts 320-380 of GLI1 mRNA to be the smallest region where CRD-BP could still physically associate with (Fig. 2). This information is invaluable for the development of inhibitors of CRD-BP-GLI1 RNA interaction for: (i) the effective design of oligonucleotides which could block the CRD-BP-GLI1 RNA interaction, (ii) the comparison between GLI1 RNA sequence and structures with that of other RNA binders which could lead to a better understanding of the RNA sequences and structural requirements for CRD-BP-RNA binding, and (iii) the use of small fluorescently labeled GLI1 RNA in fluorescent polarization assays to screen for small molecule inhibitors of CRD-BP-

Molecular Pharmacology Fast Forward. Published on April 1, 2016 as DOI: 10.1124/mol.115.102434
This article has not been copyedited and formatted. The final version may differ from this version.

GLI1 RNA interaction. With respect to the second point, the comparison of the MFOLD predicted structure of GLI1 and CD44 RNAs led us to hypothesize that the two distinct common stem loops (Fig. 3) are important for RNA interactions with CRD-BP. We therefore designed a S1 sense RNA oligonucleotide spanning the two stem loop regions of GLI1 RNA at nts 346-382 (Fig. 4), which turned out to be an effective inhibitor of the CRD-BP-GLI1 RNA interaction (Fig. 5). Our results using a number of variation of S1 RNA oligonucleotide showed that changes in the sequences and structure of the two stem loops led to a significant decrease in its effectiveness as an inhibitor (Fig. 5), further corroborating the significant role played by the two stem loops of GLI1 RNA in binding CRD-BP.

In addition to understanding the GLI1 RNA sequence and structural requirements for binding CRD-BP, we also investigated the role of each of the KH domains on CRD-BP in binding to GLI1 RNA. This was examined using KH variants of CRD-BP with a point mutation in the GXXG motif (Barnes et al., 2015). We found that the KH1 variant had significant retardation while the KH2 variant was completely unable to bind to GLI1 RNA (Fig. 6). These results are startling and in contrast to our previous findings where we demonstrated that the two mutated variants were effective binders of c-*myc* and CD44 RNAs (Barnes et al., 2015). Our results in this study, therefore, suggest that KH1 and KH2 domain of CRD-BP plays a greater role in the binding of GLI1 RNA as compared to c-*myc* and CD44 RNAs. Surprisingly, we found that all the KH double mutation variants, including KH3-4, had complete abrogation in ability to bind GLI1 RNA (Fig. 6). Again, this is in contrast to our previous findings that KH3-4 variant was an effective binder to c-*myc* and CD44 RNAs (Barnes et al., 2015). Based on these results, we propose that the other regions of the KH3 and KH4 domains play a less critical role in binding GLI1 RNA as compared to c-*myc* and CD44 RNAs, and that the GXXG motif in KH3-4 didomain play similar role as other di-domains in the binding of GLI1 RNA. Overall, our result

Molecular Pharmacology Fast Forward. Published on April 1, 2016 as DOI: 10.1124/mol.115.102434
This article has not been copyedited and formatted. The final version may differ from this version.

further corroborate the notion that CRD-BP physically interacts with different RNAs in a distinct manner, and therefore an understanding of each unique CRD-BP-RNA interaction will be important for the design of specific inhibitors of the specific CRD-BP-RNA interaction.

A previous study showed that the over-expression of CRD-BP in 293T human embryonic kidney cells led to the stabilization of GLI1 mRNA and ultimately increased GLI1 protein level, while CRD-BP knockdown by shRNA prevented β–catenin/Tcf-dependent GLI1 up-regulation and Wnt/β-catenin-dependent signaling induction of GLI1 transcriptional activity in 293T cells and NIH3T3 cells (Noubissi et al., 2009). Such results demonstrate the existence of the CRD-BP-GLI1 mRNA interaction in those cells. Furthermore, there was a positive correlation between the activation of β–catenin signaling and expression of CRD-BP and GLI1 in a panel of colorectal cancer cell lines (Noubissi et al., 2009). In this study, we knocked down CRD-BP using siRNA in two colorectal cancer cell lines HCT116 and HT29, and three breast cancer lines MCF-7, MDA-MB-231 and T47D, and showed that the selected mRNA targets of CRD-BP, including GLI1 mRNA, were suppressed (Fig. 7). These results suggest that the physical relationship between CRD-BP and its target mRNA in these cells exists. This is consistent with the model that CRD-BP binds to and protects its target mRNAs from decay. Having established that CRD-BP-GLI1 mRNA interaction exists in the five cell lines, the effect of the 2'-*O*-methyl derivative of the S1 RNA oligonucleotide on mRNA expression was evaluated. Our results show significant decrease in GLI1 mRNA level in all cell lines upon treatment with the S1 RNA oligonucleotide (Fig. 8). Although to a lesser extent, the S1 RNA oligonucleotide also significantly decreases c-*myc* and CD44 mRNA levels in all five cell lines (Fig. 8). These results suggested that the sense S1 RNA oligonucleotide designed based on specific GLI1 RNA sequences and structure to target CRD-BP-GLI1RNA interaction, has some level of specificity in inhibiting GLI1 expression. While

Molecular Pharmacology Fast Forward. Published on April 1, 2016 as DOI: 10.1124/mol.115.102434
This article has not been copyedited and formatted. The final version may differ from this version.

elucidating the exact mechanism of action of the S1 RNA oligonucleotide in cells is beyond the scope of this study, it is possible to speculate its mode of action based on *in vitro* studies and the chemical nature of the molecule. We reason that destabilization of GLI1 mRNA is not due to the RNase H pathway because the S1 RNA oligonucleotide used in this study is a sense RNA and the 2'-*O*-methyl derivative is resistant to RNase H-mediated degradation (Schneider et al., 2011). We propose that the 37-nt sense S1 RNA oligonucleotide binds to the same site on CRD-BP as the GLI1 mRNA transcripts, and thereby occludes CRD-BP from binding to GLI1 mRNA which leads to GLI1 transcript degradation. We hypothesize that this physical association also prevents c-*myc* and CD44 mRNAs from binding to CRD-BP.

Given that aberrant Hh signaling pathway is implicated in the development of a number of human cancers, efforts have focused on finding effective inhibitors for this pathway (Amakye et al., 2013). Unfortunately, most inhibitors which target the up-stream effector protein SMO have turned out to be disappointing due to the side effects produced by the SMO inhibitors and also due to the presence of so-called "non-classical" Hh activation which is SMO-independent (Amakye et al., 2013; Shevde and Samant, 2014). To this end, there has been an increase in the development of inhibitors against GLI1 function (Amakye et al., 2013) and GLI1-DNA interaction (Infante et al., 2014). One of the non-classical Hh activation pathways includes the Wnt/β-catenin signaling which involves the stabilization of GLI1 mRNA by CRD-BP (Noubissi et al., 2009). Here, our characterization of the CRD-BP-GLI1 mRNA interaction has led to the design and discovery of a 37 nts sense S1 RNA oligonucleotide which can block CRD-BP-GLI1 RNA interaction *in vitro* and significantly suppress GLI1 mRNA expression in cells. The generated knowledge of the smallest GLI1 RNA binder of CRD-BP will now allow the development of a fluorescent polarization method to rapidly screen for small molecule inhibitors of the CRD-BP-GLI1 RNA interaction. These findings together with the new information on the

Molecular Pharmacology Fast Forward. Published on April 1, 2016 as DOI: 10.1124/mol.115.102434
This article has not been copyedited and formatted. The final version may differ from this version.

important KH domains for GLI1 RNA interaction, can pave the way for the development of new inhibitors of the Hh signaling pathway which act by destabilizing GLI1 mRNA via the inhibition of the CRD-BP-GLI1 mRNA interaction.

Molecular Pharmacology Fast Forward. Published on April 1, 2016 as DOI: 10.1124/mol.115.102434
This article has not been copyedited and formatted. The final version may differ from this version.

Acknowledgments

We thank Dr. Wai Ming Li for insightful scientific discussion and valuable input on the manuscript.

Authorship Contributions

Participated in research design: Mehmood, Akhtar, Mackedenski,Wang and Lee.

Conducted experiments: Mehmood, Akhtar, Mackedenski, and Wang.

Contributed new reagents or analytic tools: Mehmood and Lee.

Performed data analysis: Mehmood, Akhtar, Mackedenski, Wang, and Lee.

Wrote or contributed to the writing of the manuscript: Lee.

Molecular Pharmacology Fast Forward. Published on April 1, 2016 as DOI: 10.1124/mol.115.102434
This article has not been copyedited and formatted. The final version may differ from this version.

References

Amakye D, Jagani Z, and Dorsch M (2013) Unraveling the therapeutic potential of the Hedgehog pathway in cancer. *Nature Med* **19:**1410-1422.

Barnes M, van Rensburg G, Li W-M, Mehmood K, Mackedenski S, Chan C-M, King DT, Miller AL, and Lee CH (2015) Molecular insights into the coding region determinant-binding protein-RNA interaction through site-directed mutagenesis in the heterogeneous nuclear ribonucleoprotein-K-homology domains. *J Biol Chem* **290:**625-639.

Bell JL, Wachter K, Muhleck B, Pazaitis N, Kohn M, Lederer M, and Huttelmaier S (2013) Insulin-like growth factor 2 mRNA-binding proteins (IGF2BPs): post-transcriptional drivers of cancer progression? *Cell Mol Life Sci* **70:**2657-2675.

Coulis CM, Lee C, Nardone V, Prokipcak RD (2000) Inhibition of c-*myc* expression in cells by targeting an RNA-protein interaction using antisense oligonucleotides. *Mol Pharmacol* **57:**485-494.

Goswami S, Tarapore RS, Strong AMP, TeSlaa JJ, Grinblet Y, Setaluri V, and Spiegelman VS (2015) MicroRNA-340-mediated degradation of microphthalmia-associated transcription factor (MITF) mRNA is inhibited by coding region determinant-binding protein (CRD-BP). *J Biol Chem* **290:**384-395.

Gu W, Wells AL, Pan F, and Singer RH (2008) Feedback regulation between zipcode binding protein 1 and β–catenin mRNAs in breast cancer cells. *Mol Cell Biol* **28:**4963-4974.

Hui CC, and Angers S (2011) Gli proteins in development and disease. *Ann Rev Cell Dev Biol* **27:**513-537.

Infante P, Mori M, Alfonsi R, Ghirga F, Aiello F, Toscano S, Ingallina C, Siler M, Cucchi D, Po A, Miele E, D'Amico D, Canettieri G, Smaele ED, Ferretti E, Screpanti I, Barretta GU, Botta

M, Gulino A, and Marcotullio LD (2014) Gli1/DNA interaction is a druggable target for Hedgehog-dependent tumors. *EMBO J* **34:**200-217.

Kato T, Hayama S, Yamabuki T, Ishikawa N, Miyamoto M, Ito T, Tsuchiya E, Kondo S, Nakamura Y, and Daigo Y (2007) Increased expression of insulin-like growth factor-II messenger RNA binding protein 1 is associated with tumor progression in patients with lung cancer. *Clin Cancer Res* **13:**434-442.

King DT, Barnes M, Thomsen D, and Lee CH (2014) Assessing specific oligonucleotides and small molecule antibiotics for the ability to inhibit the CRD-BP-CD44 RNA interaction. *PLOS ONE* **9:**e91585.

Mao C, Flavin KG, Wang S, Dodson R, Ross J, Shapiro DJ (2006) Analysis of RNA-protein interactions by a microplate-based fluorescence anisotropy assay. *Anal Biochem* **350:**222-232.

Mahapatra L, Mao C, Andruska N, Zhang C, and Shapiro DJ (2014) High-throughput fluorescence anisotropy screen for inhibitors of the oncogenic mRNA binding protein, IMP-1. *J Biomol Sceen* **19:**427-436.

Mongroo PS, Noubissi FK, Cuatrecasas M, Kalabis J, King CE, Johnstone CN, Bowser MJ, Castells A, Speigelman VS, and Rustgi AK (2011) IMP-1 displays cross-talk with K-Ras and modulates colon cancer cell survival through the novel proapoptotic protein CYFIP2. *Cancer Res* **71:**2172-2182.

Noubissi FK, Elcheva I, Bhatia N, Shakoori A, Ougolkov A, Liu J, Minamoto T, Toss J, Fuchs SY, and Spiegelman VS (2006) CRD-BP mediates stabilization of βTrCP1 and c-*myc* mRNA in response to β–catenin signaling. *Nature* **441:**898-901.

Noubissi FK, Goswami S, Sanek NA, Kawakami K, Minamoto T, Moser A, Grinblat Y, and Spiegelman VS (2009) Wnt signaling stimulates transcriptional outcome of the hedgehog pathway by stabilizing GLI1 mRNA. *Cancer Res* **69:**8572-8578.

Noubissi FK, Kim TW, Kawahara TN, Aughenbaugh WD, Berg E, Longley BJ, Athar M, and Spiegelman VS (2014) Role of CRD-BP in the growth of human basal cell carcinoma cells. *J Invest Dermatol* **134:**1718-1724.

Prokipcak RD, Herrick DJ, and Ross J (1994) Purification and properties of a protein that binds to the C-terminal coding region of human c-*myc* mRNA. *J Biol Chem* **269:**9261-9269.

Scales SJ, and de Sauvage FJ (2009) Mechanisms of Hedgehog pathway activation in cancer and implications for therapy. *Trends Pharmacol Sci* **30:**303-312.

Schmittgen TD, and Livak KJ (2008) Analyzing real-time PCR data by the comparative CT method. *Nat Protocol* **3:**1101-1108.

Schneider PN, Olthoff JT, Matthews AJ, and Houston DW (2011) Use of fully modified 2'-O-methyl antisense oligos for loss-of-function studies in vertebrate embryos. *Genesis* **49:**117-123.

Shevde LA, and Samant RS (2014) Nonclassical Hedgehog-GLI signaling and its clinical implications. *Int J Cancer* **135:**1-6.

Sparanese D, and Lee CH (2007) CRD-BP shields c-*myc* and MDR-1 RNA from endonucleolytic attack by a mammalian endoribonuclease. *Nucleic Acid Res* **35:**1209-1221.

Stohr N, Kohn M, Lederer M, Glab M, Reinke C, Singer R.H, and Huttelmaier S (2012) IGF2BP1 promotes cell migration by regulating MK5 and PTEN signaling. *Genes Dev* **26:**176-189.

Tessier CR, Doyle GA, Clark BA, Pitot HC, and Ross J (2004) Mammary tumor induction in transgenic mice expressing an RNA-binding protein. *Cancer Res* **64:**209-214.

Vikessa J, Hansen TVO, Jonson L, Borup R, Wewer UM, Christiansen J, and Nielsen FC (2006) RNA-binding IMPs promote cell adhesion and invadopodia formation. *EMBO J* **25:**1456-1468.

Zuker M (2003) Mfold web server for nucleic acid folding and hybridization prediction. *Nucleic Acids Res* **15:**3406-3415.

Footnotes

This research was supported by the Natural Sciences & Engineering Research Council [Discovery Grant 227158].

Molecular Pharmacology Fast Forward. Published on April 1, 2016 as DOI: 10.1124/mol.115.102434
This article has not been copyedited and formatted. The final version may differ from this version.

Figure Legends

Fig. 1. Schematic diagrams for mapping the binding site on GLI1 mRNA by CRD-BP. Five fragments of DNA corresponding to GLI1 cDNAs nts 36-990 (A) and four DNA fragments corresponding to nts 230-420 (B and C) were PCR-amplified with the appropriate 5' primer containing T7 promoter sequence. [^{32}P] RNA was prepared from each template and analyzed by electrophoretic mobility shift assay for CRD-BP binding. + indicates binding; - indicates no binding.

Fig. 2. Mapping the CRD-BP binding site on GLI1 mRNA using electrophoretic mobility shift assay. A, 5 different fragments (nts 36-230, 230-420, 420-610, 610-800, and 800-990) of [^{32}P] GLI1 RNA (13 nM) covering nts 36-990 of GLI1 cDNA were incubated with various concentrations of recombinant CRD-BP as shown. B, 4 different 3' truncated fragments (nts 230-380, 230-330, 230-300, and 230-275) of [^{32}P] GLI1 RNA covering nts 230-420 of GLI1 cDNA were incubated with various concentrations of recombinant CRD-BP as shown. C, 4 different 5' truncated fragments (nts 270-420. 320-420, 350-420, and 375-420) of [^{32}P] GLI1 RNA covering nts 230-420 of GLI1 cDNA were incubated with various concentrations of recombinant CRD-BP. D, [^{32}P] GLI1 RNA nts 320-380 (13 nM) was incubated with various concentrations of CRD-BP as shown. [^{32}P] c-*myc* RNA nts 1705-1886 was used as the positive control as shown in (A) and (B). In each gel, free RNA and CRD-BP-bound RNA are indicated.

Fig. 3. Predicted RNA secondary structure of GLI1 and CD44 RNAs. The predicted secondary structures of GLI1 RNA nts 301-380 (left panel) and CD44 RNA nts 2862-2930 (right panel) were generated using the MFOLD program (Zuker 2003).

Molecular Pharmacology Fast Forward. Published on April 1, 2016 as DOI: 10.1124/mol.115.102434
This article has not been copyedited and formatted. The final version may differ from this version.

Fig. 4. Predicted secondary structures of oligonucleotides used against CRD-BP-GLI1 RNA interaction. The predicted secondary structures of DNA Oligo D1 and RNA oligonucleotides S1 to S8 were generated using the MFOLD program (Zuker 2003).

Fig. 5. Inhibition of the CRD-BP-GLI1 RNA interaction by specific oligonucleotides as determined by electrophoretic mobility shift assay (EMSA). A, Purified recombinant CRD-BP (300 nM) was incubated with [^{32}P] GLI1 RNA nts 230-420 in the presence of different concentrations (μM) of GLI1 RNA nts 320-380, D1 DNA Oligo or S1 RNA oligonucleotide. B, As in (A) different concentrations of competitor RNA oligonucleotides S1 to S8 were added to the EMSA reaction containing CRD-BP and [^{32}P] GLI1 RNA nts 230-420. Lane 1 on each gel has no CRD-BP added. Lane 2 on each gel has 300 nM CRD-BP added but had no competitor added.

Fig. 6. Binding profile of CRD-BP and its point mutation variants on GLI1 RNA. A, Electrophoretic mobility gel-shift assay on the binding of purified recombinant WT CRD-BP and its point mutation variants to [^{32}P] GLI1 RNA nts 230-420. Various concentrations of proteins, as indicated, were incubated with 40 nM of the radiolabeled GLI1 RNA. The positions of protein-RNA complexes (Bound) and free RNA are indicated. Samples within each panel indicate the same experiment. B, A summary of dissociation constants (K_d) of the WT CD-BP and its variants. The K_d values were taken from saturation binding curves (n = 4). The single asterisk indicates that the p-value is less than 0.05 (P = 0.0317) based on Student's t-test in comparing to the K_d of WT CRD-BP. The double asterisks indicate that there was significant reduction or no binding and hence K_d could not be determined.

Molecular Pharmacology Fast Forward. Published on April 1, 2016 as DOI: 10.1124/mol.115.102434
This article has not been copyedited and formatted. The final version may differ from this version.

Fig. 7. Effect of knocking down CRD-BP on GLI1 and other mRNA expression in breast and colon cancer cell lines. Colon cancer cells (HCT116 and HT29) and breast cancer cells (MCF-7, MDA-MB-231, and T47D) were plated and transfected with 20 nM of dsiRNA-CRD-BP or the negative control duplex NC1 as described in the Materials and Methods. Total RNA extracted was subjected to quantitative real-time PCR for measurements of GLI1, c-*myc*, CD44, and β–actin mRNAs. The steady-state mRNA levels of GLI1, c-*myc*, and CD44 were normalized to the reference gene β-actin. Data shown are expressed as relative to the negative control NC1 which is taken as 1.0, and were averaged from five biological replicates (n = 5) with S.E. as error bars. One-way ANOVA was performed as statistical analysis. Asterisk indicates results are significantly different from the negative control, NC1.

Fig. 8. Effect of S1 RNA oligonucleotide on GLI1 and other mRNA expression in breast and colon cancer cell lines. Colon cancer cells (HCT116 and HT29) and breast cancer cells (MCF-7, MDA-MB-231, and T47D) were plated and transfected with 100 nM of 2'-*O*-methyl derivative of S1 RNA oligonucleotide as described in the Materials and Methods. Total RNA extracted was subjected to quantitative real-time PCR for measurements of GLI1, c-*myc*, CD44, and β–actin mRNAs. The steady-state mRNA levels of GLI1, c-*myc*, and CD44 were normalized to the reference gene β-actin. Data shown are expressed as relative to the negative control S4 RNA oligonucleotide which is taken as 1.0, and were averaged from five biological replicates (n = 5) with S.E. as error bars. One-way ANOVA was performed as statistical analysis. Asterisk indicates results are significantly different from the negative control, Oligo S4.

Molecular Pharmacology Fast Forward. Published on April 1, 2016 as DOI: 10.1124/mol.115.102434
This article has not been copyedited and formatted. The final version may differ from this version.

Tables

TABLE 1

Sequences of oligonucleotides used in the competitive EMSA

Name	Sequences (5’ to 3’)
D1	CCAGCTCCCT CGTAGCTTTC ATCAACTCGCGATGCAC
S1	CCAGCUCCCUCGUAGCUUUCAUCAACUCGCGAUGCAC
S2	CCGGACCCCUCGUAGCUUUCAUCAACUCGCGAUGCAC
S3	CCAGCUCCCUCGUAGCUUUCAUCAACUCGCCACCCCC
S4	CCAGCUCCCUAGCUUUUUUCAUCAACUCGCGAUGCAC
S5	CCAGCUCCCUCGUAGCUUUCAUCAACUGAUGCACCCG
S6	CCCCCAGCUCCCUAGCUUUCAUCAACUCGCGAUGCAC
S7	CCCUGCCCCUCGUGCAGUUUCUAAACUCGCUAGACAC
S8	CCAGCUGAACGAAAGCUUUCAUCUUAACCCGAUGCAC

Molecular Pharmacology Fast Forward. Published on April 1, 2016 as DOI: 10.1124/mol.115.102434
This article has not been copyedited and formatted. The final version may differ from this version.

TABLE 2

Sequences of primers used for amplifying GLI1 DNA fragments

Name	Sequences (5' to 3')
GLI1 36-231	Forward: GGATCCTAATACGACTCACTATAGGGCCATGTTCAACTCGATG Reverse: CCTCGGTGCAGCTGTTGG
GLI1 230-420	Forward: GGATCCTAATACGACTCACTATAGGGGGCCCACTCTTTTCTTC Reverse: TGCCAATGGAGAGATGAC
GLI1 420-610	Forward: GGATCCTAATACGACTCACTATAGGACCATGAGCCCATCTCTG Reverse: CGGCACTTGCCAACCAGC
GLI1 610-800	Forward: GGATCCTAATACGACTCACTATAGGGGGAGGAACCCTTGGAAG Reverse: GTGCACCAGCTGCTCTTG
GLI1 800-990	Forward: GGATCCTAATACGACTCACTATAGGCCACATCAACAGCGAGCA Reverse: GGTTTTCGAGGCGTGAGT
GLI1 230-380	Forward: As above for GLI1 230-420 Reverse: GCATCGCGAGTTGATGAA
GLI1 230-330	Forward: As above for GLI1 230-420 Reverse: CCGTCTGCAGGTCCAGGC
GLI1 230-300	Forward: As above for GLI1 230-420 Reverse: GAGGTGAGATGGACAGTG
GLI1 230-275	Forward: As above for GLI1 230-420 Reverse: CTTGGTCAACTTGACTGC
GLI1 270-420	Forward: GGATCCTAATACGACTCACTATAGGACCAAGAAGCGGGCACTG Reverse: As above for GLI1 230-420
GLI1 320-420	Forward: GGATCCTAATACGACTCACTATAGGCCTGCAGACGGTTATCCG Reverse: As above for GLI1 230-420
GLI1 350-420	Forward: GGATCCTAATACGACTCACTATAGGCTCCCTCGTAGCTTTCAT Reverse: As above for GLI1 230-420
GLI1 375-420	Forward: GGATCCTAATACGACTCACTATAGGCGATGCACATCTCCAGGA Reverse: As above for GLI1 230-420
GLI1 320-380	Forward: As above for GLI1 320-420 Reverse: As above for GLI1 230-380

T7 RNA promoter sequences are underlined

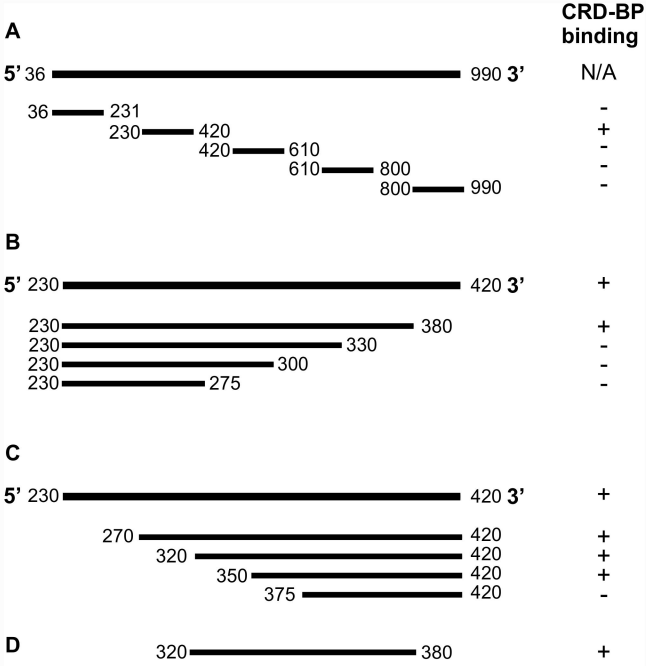
CRD-BP binding
A
5' 36 990 3'
N/A
36 231
230 420
420 610
610 800
800 990
B
5' 230 420 3'
230 380
230 330
230 300
230 275
C
5' 230 420 3'
270 420
320 420
350 420
375 420
D
320 380

Figure 1

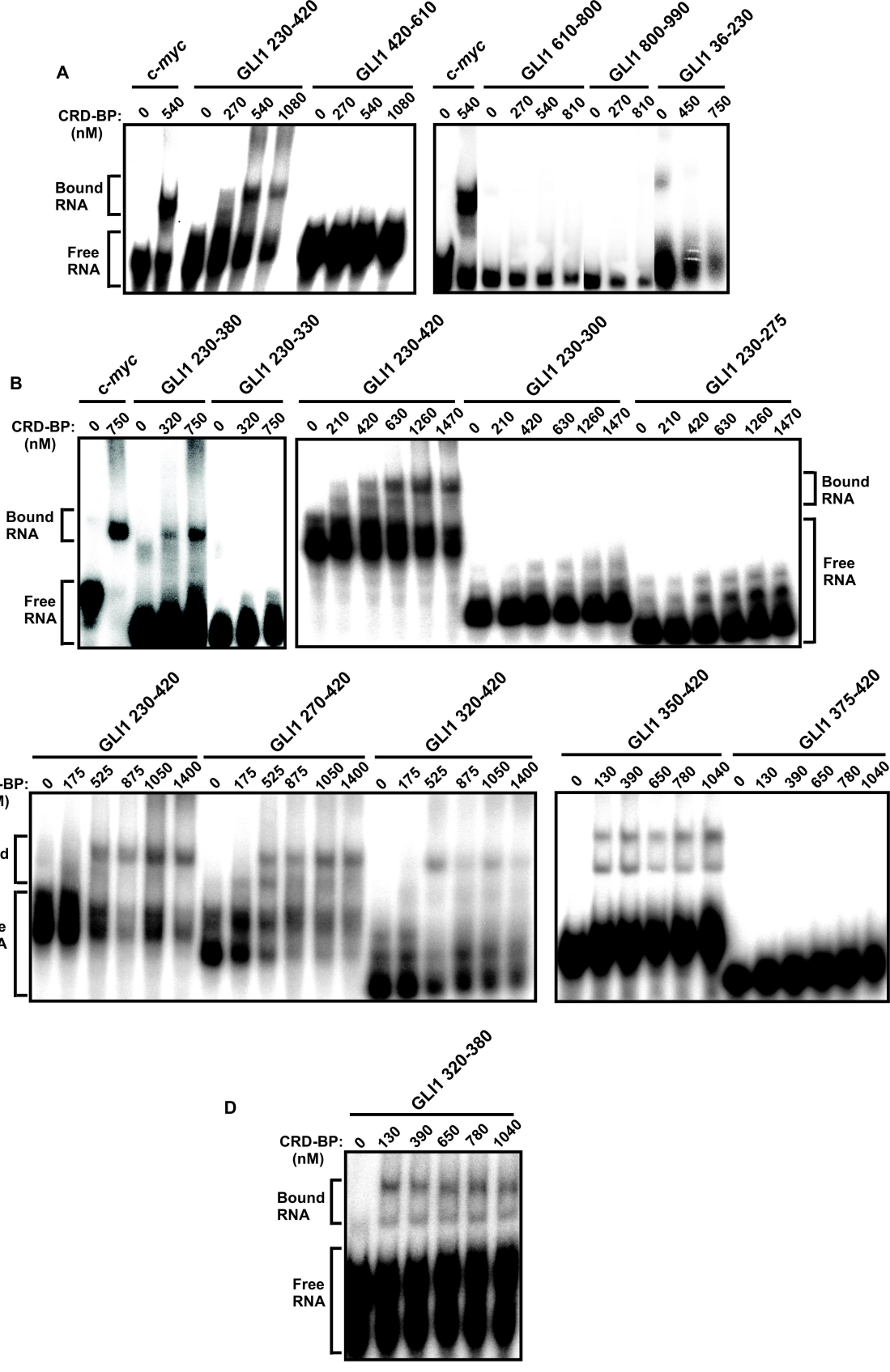
A
c-myc
GLI1 230-420
GLI1 420-610
c-myc
GLI1 610-800
GLI1 800-990
GLI1 36-230
CRD-BP: (nM)
0 540
0 270 540 1080
0 270 540 1080
0 540
0 270 540 810
0 270 810
0 450 750
Bound RNA
Free RNA
B
c-myc
GLI1 230-380
GLI1 230-330
GLI1 230-420
GLI1 230-300
GLI1 230-275
CRD-BP: (nM)
0 750
0 320 750
0 320 750
0 210 420 630 1260 1470
0 210 420 630 1260 1470
0 210 420 630 1260 1470
Bound RNA
Free RNA
C
GLI1 230-420
GLI1 270-420
GLI1 320-420
GLI1 350-420
GLI1 375-420
CRD-BP: (nM)
0 175 525 875 1050 1400
0 175 525 875 1050 1400
0 175 525 875 1050 1400
0 130 390 650 780 1040
0 130 390 650 780 1040
Bound RNA
Free RNA
D
GLI1 320-380
CRD-BP: (nM)
0 130 390 650 780 1040
Bound RNA
Free RNA

Figure 2

GLI1

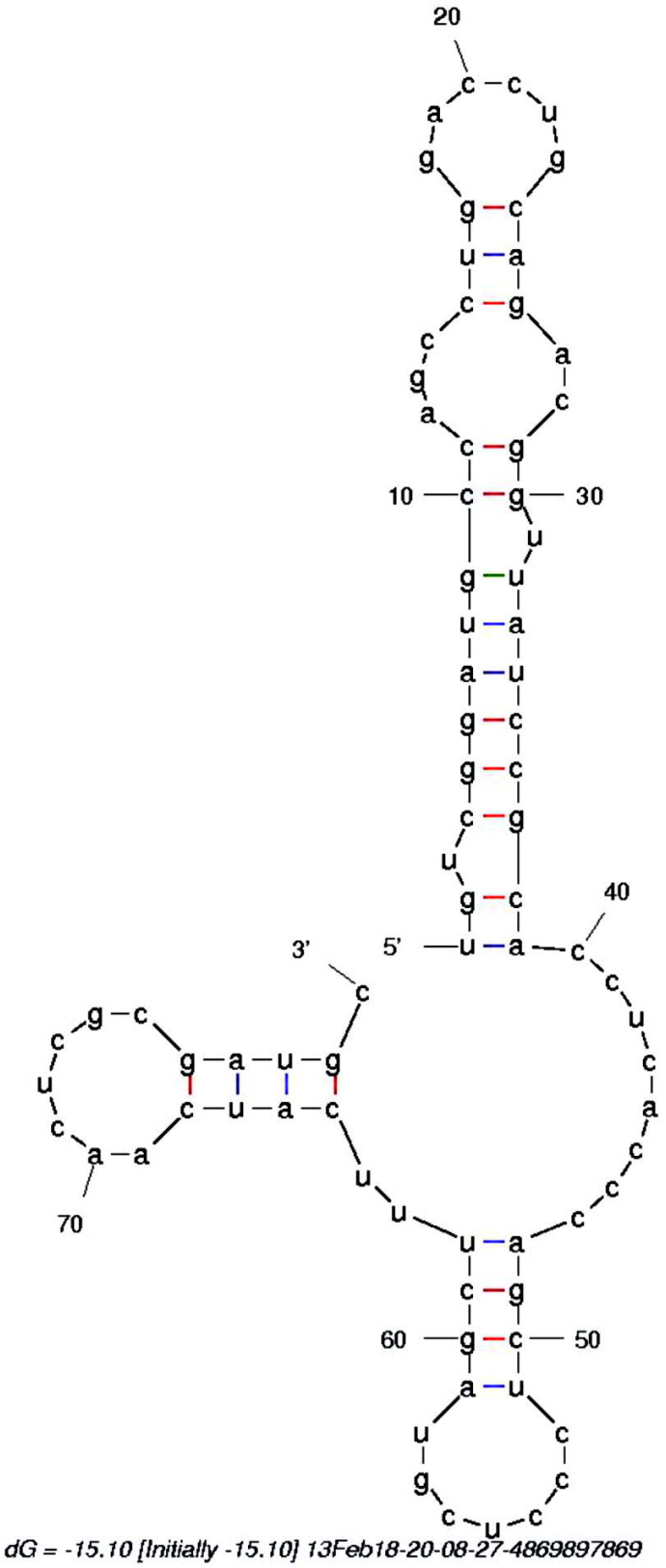

CD44

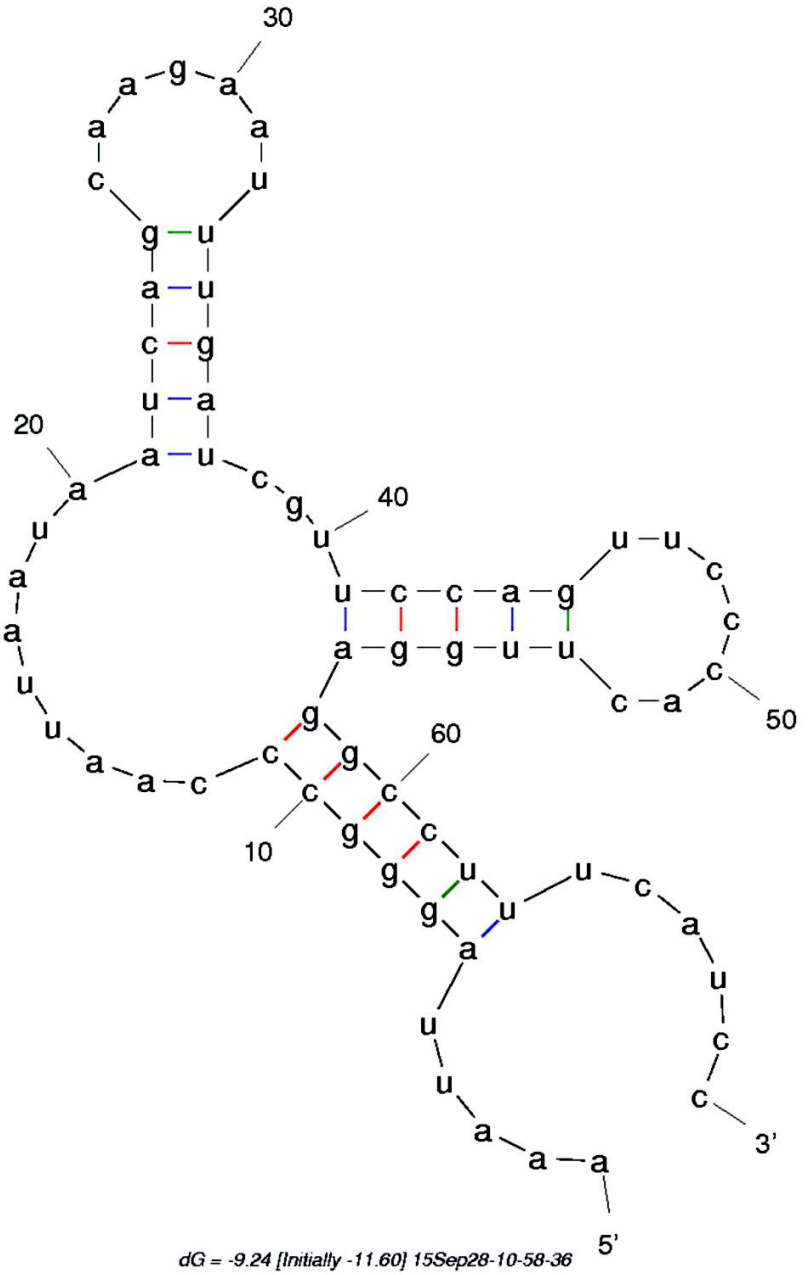

Figure 3

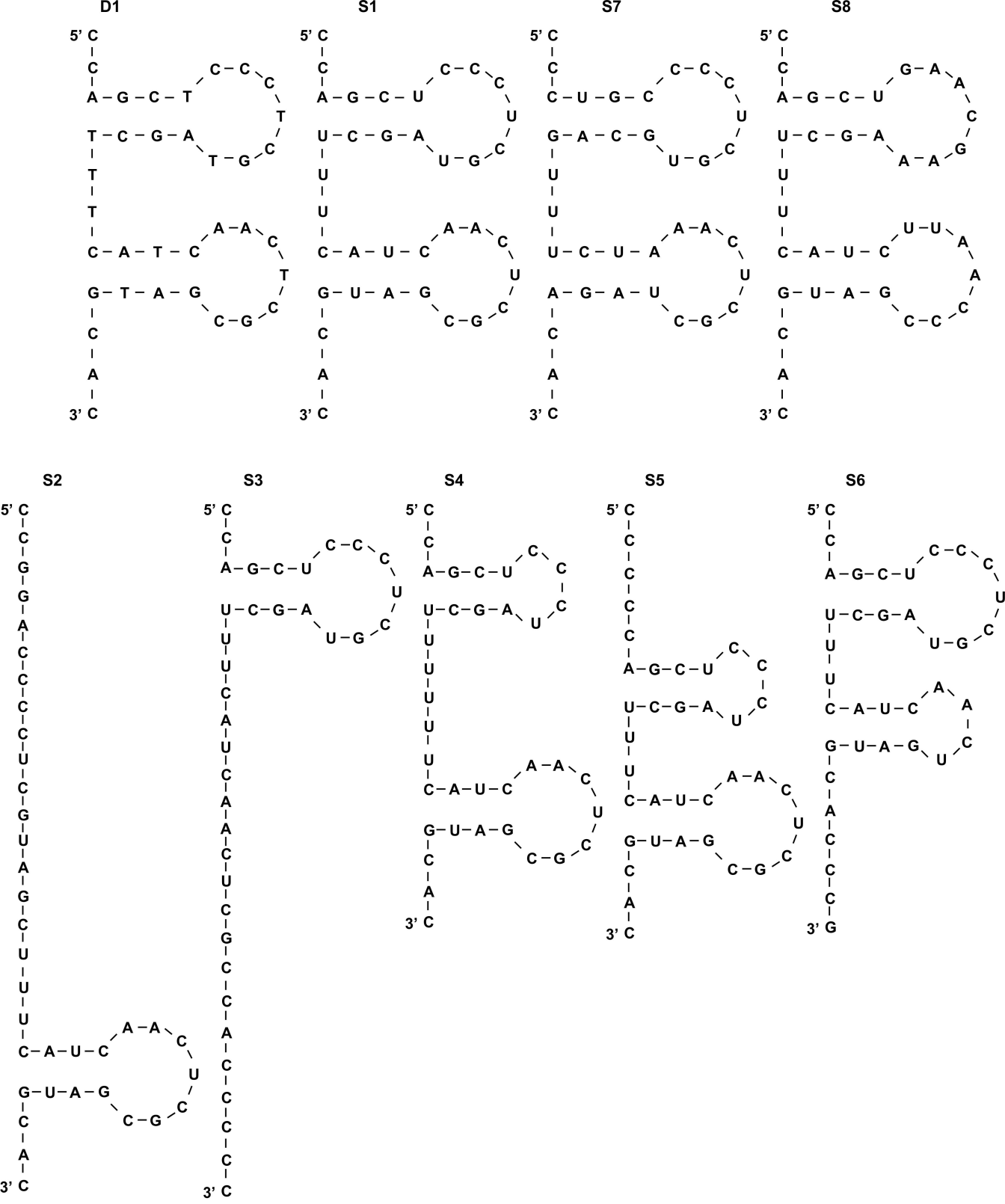

Figure 4

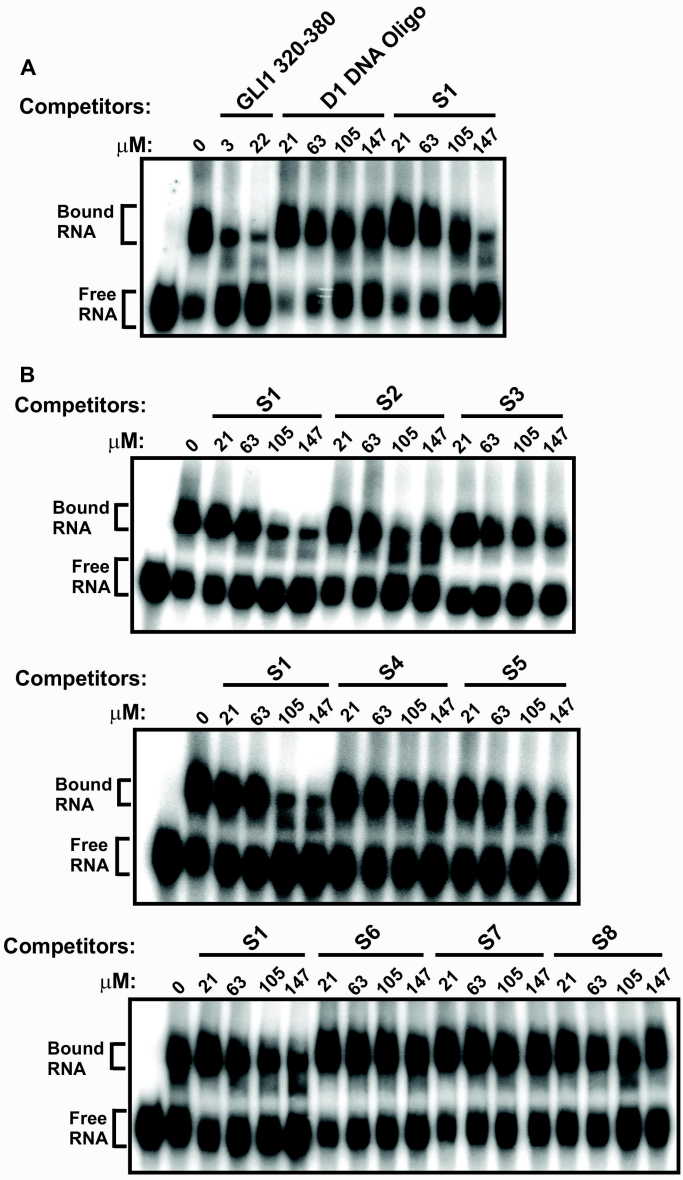
A
Competitors:
GLI1 320-380
D1 DNA Oligo
S1
μM:
0 3 22 21 63 105 147 21 63 105 147
Bound RNA
Free RNA
B
Competitors:
S1
S2
S3
μM:
0 21 63 105 147 21 63 105 147 21 63 105 147
Bound RNA
Free RNA
Competitors:
S1
S4
S5
μM:
0 21 63 105 147 21 63 105 147 21 63 105 147
Bound RNA
Free RNA
Competitors:
S1
S6
S7
S8
μM:
0 21 63 105 147 21 63 105 147 21 63 105 147 21 63 105 147
Bound RNA
Free RNA

Figure 5

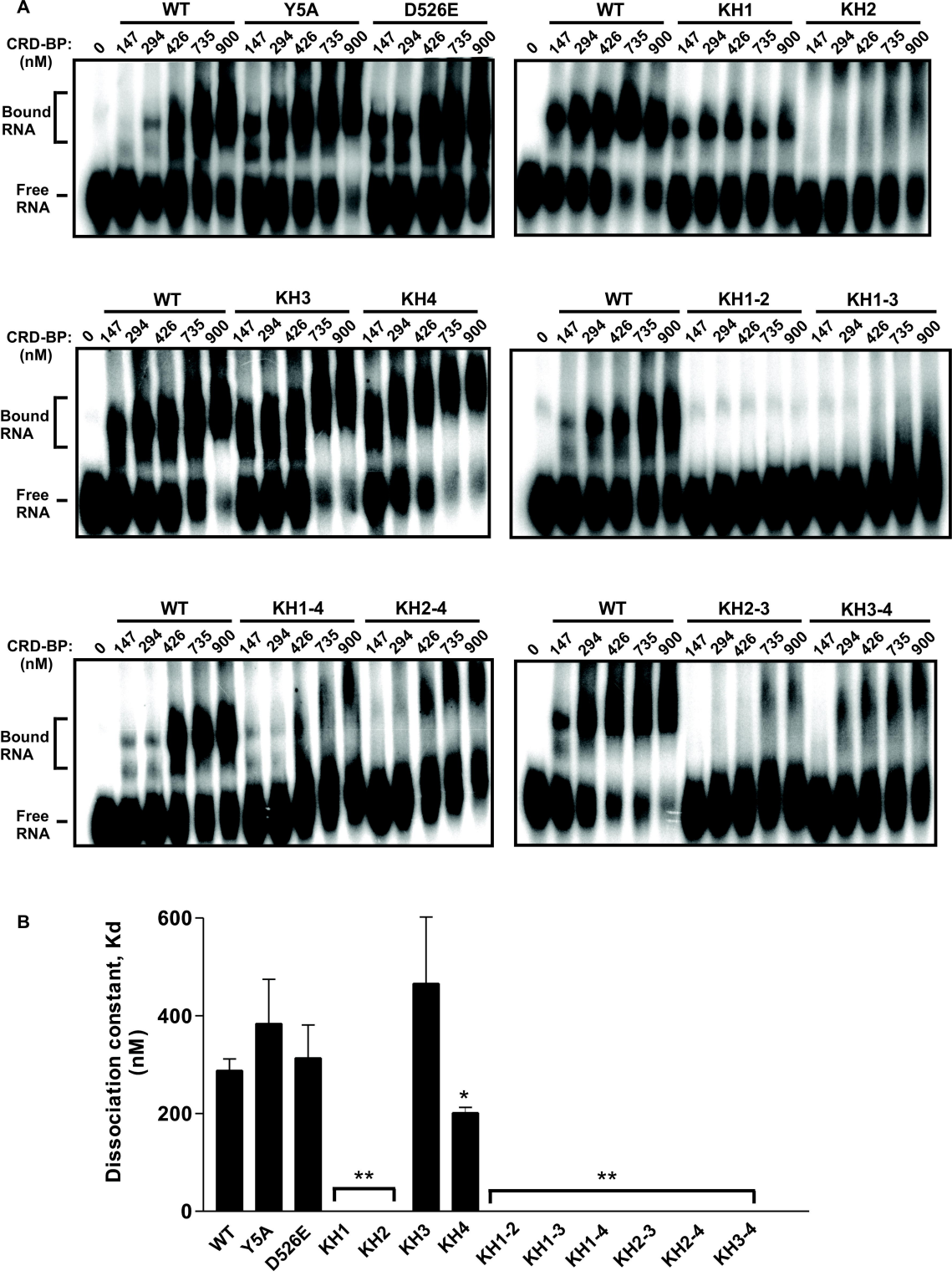
A
WT
Y5A
D526E
KH1
KH2
KH3
KH4
KH1-2
KH1-3
KH1-4
KH2-4
KH2-3
KH3-4
CRD-BP: (nM)
0
147
294
426
735
900
Bound RNA
Free RNA
B
Dissociation constant, Kd (nM)
600
400
200
0
*
**
**
WT
Y5A
D526E
KH1
KH2
KH3
KH4
KH1-2
KH1-3
KH1-4
KH2-3
KH2-4
KH3-4

Figure 6

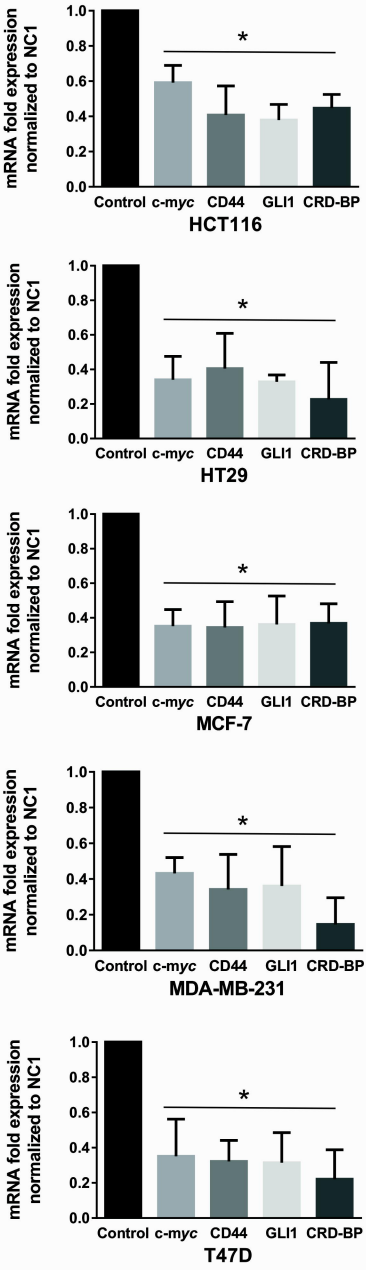
mRNA fold expression normalized to NC1
1.0
0.8
0.6
0.4
0.2
0.0
*
Control
c-myc
CD44
GLI1
CRD-BP
HCT116
HT29
MCF-7
MDA-MB-231
T47D

Figure 7

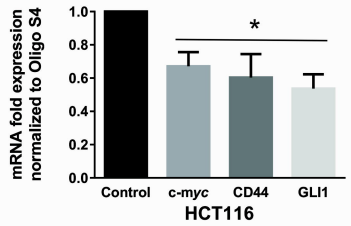
mRNA fold expression normalized to Oligo S4
1.0
0.8
0.6
0.4
0.2
0.0
*
Control
c-myc
CD44
GLI1
HCT116

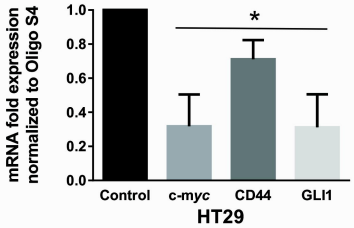
mRNA fold expression normalized to Oligo S4
1.0
0.8
0.6
0.4
0.2
0.0
*
Control
c-myc
CD44
GLI1
HT29

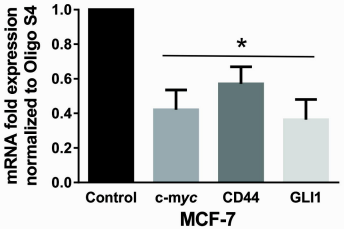
mRNA fold expression normalized to Oligo S4
1.0
0.8
0.6
0.4
0.2
0.0
*
Control
c-myc
CD44
GLI1
MCF-7

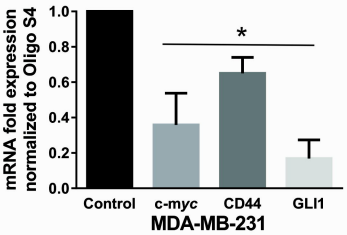
mRNA fold expression normalized to Oligo S4
1.0
0.8
0.6
0.4
0.2
0.0
*
Control
c-myc
CD44
GLI1
MDA-MB-231

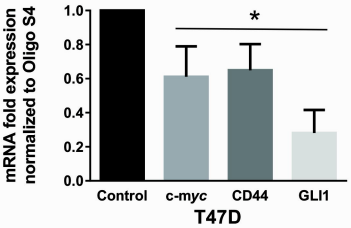
mRNA fold expression normalized to Oligo S4
1.0
0.8
0.6
0.4
0.2
0.0
*
Control
c-myc
CD44
GLI1
T47D

Figure 8